Comparative Study of Homochiral and Racemic Chiral Metal-Organic Frameworks Built from Camphoric Acid

Jian Zhang,[†] Yuan-Gen Yao,[‡] and Xianhui Bu*,[†]

Department of Chemistry and Biochemistry, California State University, Long Beach, 1250 Bellflower Boulevard, Long Beach, California 90840, and Fujian Institute of Research on the Structure of Matter, The Chinese Academy of Sciences, Fuzhou, Fujian 350002, China

Received June 24, 2007. Revised Manuscript Received July 25, 2007

The study of the crystallization of homochiral or racemic chiral framework materials from enantiopure or racemic ligands is an important step for the rational design of crystalline homochiral materials. The self-assembly of extended frameworks in the presence of enantiopure or racemic ligands is regulated by the differing symmetry requirements of the ligand. By employing both enantiopure and racemic ligands as cross-linking ligands, we have prepared three homochiral and three racemic chiral compounds and their synthesis and structural and topological properties are presented here. It is shown that depending on the chemical compositions and framework topologies, the effect of the ligand handedness on the resulting crystal structure can vary greatly. The ligand handedness can have negligible effect on the crystallization, which leads to an interesting example of two pairs of isostructural achiral and homochiral structures with two types of six-connected nets. In another example reported here, the racemic chiral−chiral conversion is accompanied by the twofold supercell formation with homochiral layers and racemic chiral layers pillared in two unique patterns.

Introduction

Crystalline microporous and open-framework materials with homochiral framework are of great interest because of their potential applications in enantioselective processes such as catalysis and separation.[1] It is generally difficult to synthesize a homochiral solid with purely inorganic framework (similar to quartz) because of the lack of suitable inorganic chiral building blocks. Thus, homochiral inorganic framework materials generally come from the spatial organization of achiral precursors and such organization usually results in the formation both right- and left-handed forms.[2] As a result, the bulk samples is usually a racemic mixture, even though under special circumstances a spontaneous resolution into a particular handedness is possible.[3]

Recent successes with metal-organic framework materials (MOFs) have opened up new routes toward the synthesis of homochiral solids.[4,5] One of the most successful methods for the synthesis of homochiral materials is to use enantiopure chiral building blocks for the construction of extended frameworks.[1a−c] To achieve a more rational design of homochiral framework materials, it is necessary to understand and be able to predict the types of framework topologies that may be realized with the enantiopure building blocks. This is not a trivial task because much of the earlier topological studies are based on achiral crystalline materials and the crystallization of homochiral solids have some fundamental differences from that of achiral (or racemic chiral) solids because of the inherent symmetry restrictions imposed on the crystallization of homochiral solids (i.e., no inversion axes permitted).

In this work, we are interested in two aspects of the formation of homochiral solids: (1) synthetic and structural conditions under which racemic chiral solids can be directly converted into homochiral solids by a simple change in the building blocks *without* a concurrent change in the crystal structure and/or the framework topology and (2) how a change in the chirality of the basic building block induces a crystal structural (or topological) change in racemic chiral and homochiral solids. To help gain insights into these two aspects, we have performed a comparative study on the chirality effects of enantiopure and racemic ligands. We

---

* To whom correspondence should be addressed. E-mail: xbu@csulb.edu.
[†] California State University, Long Beach.
[‡] Fujian Institute of Research on the Structure of Matter, CAS.

(1) (a) Seo, J. S.; Whang, D.; Lee, H.; Jun, S. I.; Oh, J.; Jeon, Y. J.; Kim, K. *Nature* **2000**, *404*, 982. (b) Cui, Y.; Evans, O. R.; Ngo, H. L.; White, P. S.; Lin, W. *Angew. Chem., Int. Ed.* **2002**, *41*, 1159. (c) Vaidhyanathan, R.; Bradshaw, D.; Rebilly, J.-N.; Barrio, J. P.; Gould, J. A.; Berry, N. G.; Rosseinsky, M. J. *Angew. Chem., Int. Ed.* **2006**, *45*, 6495. (d) Kepert, C. J.; Prior, T. J.; Rosseinsky, M. J. *J. Am. Chem. Soc.* **2000**, *122*, 5158. (e) Bradshaw, D.; Prior, T. J.; Cussen, E. J.; Claridge, J. B.; Rosseinsky, M. J. *J. Am. Chem. Soc.* **2004**, *126*, 6106.

(2) (a) Lin, H.-M.; Lii, K.-H. *Inorg. Chem.* **1998**, *37*, 4220. (b) Li, K.-H.; Chen, C.-Y. *Inorg. Chem.* **2000**, *39*, 3374. (b)Wang, Y.; Yu, J.; Du, Y.; Shi, Z.; Zou, Y.; Xu, R. *J. Chem. Soc., Dalton Trans.* **2002**, 4060.

(3) (a) Ezuhara, T.; Endo, K.; Aoyama, Y. *J. Am. Chem. Soc.* **1999**, *121*, 3279. (b) Lin, Z.; Slawin, A. M. Z.; Morris, R. E. *J. Am. Chem. Soc.* **2007**, *129*, 4880.

(4) (a) Hagrman, P. J.; Hagrman, D.; Zubieta, J. *Angew. Chem., Int. Ed.* **1999**, *38*, 2638. (b) Khlobystov, A. N.; Blake, A. J.; Champness, N. R.; Lemenovskii, D. A.; Majouga, A. G.; Zyk, N. V.; Schröder, M. *Coord. Chem. Rev.* **2001**, *222*, 155. (c) Moulton, B.; Zaworotko, M. J. *Chem. Rev.* **2001**, *101*, 1629. (d) Yaghi, O. M.; O'Keeffe, M.; Ockwig, N. W.; Chae, H. K.; Eddaoudi, M.; Kim, J. *Nature* **2003**, *423*, 705. (e) Ockwig, N. W.; Delgado-Friederichs, O.; O'Keeffe, M.; Yaghi, O. M. *Acc. Chem. Res.* **2005**, *38*, 176. (f) O'Keefe, M.; Eddaoudi, M.; Li, H.; Reineke, T.; Yaghi, O. M. *J. Solid State Chem.* **2000**, *152*, 3.

(5) (a) Anokhina, E. V.; Jacobson, A. J. *J. Am. Chem. Soc.* **2004**, *126*, 3044. (b) Zhang, Y.; Saha, M. K.; Bernal, I. *CrystEngComm* **2003**, *5*, 34.

10.1021/cm071689a CCC: $37.00

reported earlier that an achiral material with the four-connected diamond-type topology can be readily converted into a homochiral one with a change in the chirality of the basic building block.[6] Obviously, the ability to create the direct conversion from an achiral framework into the homochiral one without any concurrent change in crystal structures or topology offers a convenient path for the rational design of homochiral materials. We therefore are interested in exploring the feasibility of extending this method to other chemical compositions and framework topologies. Reported here is a comparative study of homochiral and racemic chiral six-connected self-penetrating frameworks synthesized from enantiopure and racemic camphoric acid.

Racemic chiral and homochiral solids reported here are prepared by using a dual-ligand synthetic strategy that integrates transition-metal cations, D-(+)-camphoric acid (=D-H_2Cam) (or the DL-form for comparative purpose) and bipyridine ligands. By incorporation of the enantiopure D-Cam ligand, the resulting frameworks should be homochiral. The auxiliary bipyridine ligands serve to cross-link chiral metal carboxylate layers into pillared open-framework architectures. This synthetic strategy involving two complementary ligands has been widely used in the synthesis of metal-organic framework materials. However, there has been rather limited effort on the use of this method for the synthesis of homochiral frameworks.

In the synthesis of open-framework materials, a common phenomenon is the interpenetration of two or more nets, which is the polymeric counterpart of catenane-type molecular structures. The most commonly observed interpenetration occurs with the four-connected diamond net. More recently, a completely different phenomenon, self-penetrating (self-catenated or polyknotting) networks, has attracted attentions.[7−11] Unlike interpenetration that involves two or more nets, the self-catenation involves only one net (comparable to molecular knots). The first examples of 3-D self-penetrating frameworks within coordination polymers were described by Robson and co-workers,[9] and later some other connectivity nets with self-penetrating behavior have been found, such as three-connected 12^3 net,[4f] four-connected 8^6 net,[10] six-connected $4^8.6^6.8$ and 4^86^7 nets,[7] 8-connected $4^{24}.5.6^3$ and $4^{20}.6^8$ nets.[11] However, to our knowledge, homochiral self-penetrating networks have been rarely reported so far.

Here we report three homochiral compounds, [M_2(D-Cam)$_2$(4,4′-bpy)]$_n$ (**1^c**, M = Cu; **2^c**, M = Zn; 4,4′-bpy = 4,4′-bipyridine; superscript "c" means chiral) and [Cd_4(D-Cam)$_4$(bpe)$_3$]$_n$ (**3^c**, bpe = *trans*-1,2-bis(4-pyridyl)-ethylene), together with three racemic chiral compounds [M_2(DL-Cam)$_2$-(4,4′-bpy)]$_n$ (**1^a**, M = Cu; **2^a**, M = Zn; superscript "a" means achiral) and [Cd_2(DL-Cam)$_2$(bpe)$_{3/2}$]$_n$ (**3^a**). They consist of homochiral or racemic chiral metal carboxylate layers pillared by bipyridine ligands to form two types of unusual three-dimensional six-connected self-penetrating architectures.

Experimental Section

Synthesis. *(a) [Cu_2(D-Cam)$_2$(4,4′-bpy)]$_n$ (**1^c**).* $Cu(NO_3)_2{\cdot}3H_2O$ (0.1545 g), Na_2CO_3 (0.0518 g), 4,4′-bipyridine (0.0923 g), and D-(+)-camphoric acid (0.0975 g) in a molar ratio of 2:1:1:1 and distilled water (8.3729 g) were mixed in a 23 mL Teflon cup and the mixture was stirred for 20 min. The vessel was then sealed and heated at 120 °C for 2 days. The autoclave was subsequently allowed to cool to room temperature. The final pH was 5.73. Plate-shaped transparent green crystals were obtained.

*(b) [Zn_2(D-Cam)$_2$(4,4′-bpy)]$_n$ (**2^c**).* $Zn(NO_3)_2{\cdot}6H_2O$ (0.2217 g), Na_2CO_3 (0.0476 g), 4,4′-bipyridine (0.0791 g), and D-(+)-camphoric acid (0.1110 g) in a molar ratio of 1.5:1:1:1 and distilled water (8.7244 g) were mixed in a 23 mL Teflon cup and the mixture was stirred for 20 min. The vessel was then sealed and heated at 120 °C for 2 days. The autoclave was subsequently allowed to cool to room temperature. Transparent colorless crystals were obtained.

*(c) [Cd_4(D-Cam)$_4$(bpe)$_3$]$_n$ (**3^c**).* $Cd(NO_3)_2{\cdot}6H_2O$ (0.2189 g), Na_2CO_3 (0.0477 g), *trans*-1,2-bis(4-pyridyl)-ethylene (0.0500 g), and D-(+)-camphoric acid (0.1036 g) in a molar ratio of 1.5:1:1:1 and distilled water (8.49706 g) were mixed in a 23 mL Teflon cup and the mixture was stirred for 20 min. The vessel was then sealed and heated at 120 °C for 2 days. The autoclave was subsequently allowed to cool to room temperature. Plate-shaped transparent colorless crystals were obtained.

*(d) [Cu_2(DL-Cam)$_2$(4,4′-bpy)]$_n$ (**1^a**).* $Cu(NO_3)_2{\cdot}3H_2O$ (0.1745 g), Na_2CO_3 (0.0505 g), 4,4′-bipyridine (0.0825 g), and DL-camphoric acid (0.1075 g) in a molar ratio of 2:1:1:1 and distilled water (8.1236 g) were mixed in a 23 mL Teflon cup and the mixture was stirred for 20 min. The vessel was then sealed and heated at 120 °C for 2 days. The autoclave was subsequently allowed to cool to room temperature. Plate-shaped transparent green crystals were obtained.

*(e) [Zn_2(DL-Cam)$_2$(4,4′-bpy)]$_n$ (**2^a**).* $Zn(NO_3)_2{\cdot}6H_2O$ (0.2115 g), Na_2CO_3 (0.0502 g), 4,4′-bipyridine (0.0803 g), and DL-camphoric acid (0.1023 g) in a molar ratio of 1.5:1:1:1 and distilled water (8.0006 g) were mixed in a 23 mL Teflon cup and the mixture was stirred for 20 min. The vessel was then sealed and heated at 120 °C for 2 days. The autoclave was subsequently allowed to cool to room temperature. Colorless crystals were obtained.

*(f) [Cd_2(DL-Cam)$_2$(bpe)$_{3/2}$]$_n$ (**3^a**).* $Cd(NO_3)_2{\cdot}6H_2O$ (0.2546 g), Na_2CO_3 (0.0523 g), *trans*-1,2-bis(4-pyridyl)-ethylene (0.0512 g), and DL-camphoric acid (0.1123 g) in a molar ratio of 1.5:1:1:1 and distilled water (8.0089 g) were mixed in a 23 mL Teflon cup and the mixture was stirred for 20 min. The vessel was then sealed and heated at 120 °C for 2 days. The autoclave was subsequently allowed to cool to room temperature. Plate-shaped transparent colorless crystals were obtained.

Single-Crystal Structure Analysis. Each crystal was glued to a thin glass fiber with epoxy resin and mounted on a Bruker APEX II diffractometer equipped with a fine focus, 2.0 kW sealed tube X-ray source (Mo Kα radiation, $\lambda = 0.71073$ Å) operating at 50 kV and 30 mA. The empirical absorption correction was based on equivalent reflections and other possible effects such as absorption by the glass fiber were simultaneously corrected. Each structure was solved by direct methods followed by successive difference

---

(6) Zhang, J.; Bu, X. *Angew. Chem. Int. Ed.* **2007**, *46*, 6115.

(7) (a) Long, D.-L.; Hill, R. J.; Blake, A. J.; Champness, N. R.; Hubberstey, P.; Wilson, C.; Schröder, M. *Chem. Eur. J.* **2005**, *11*, 1384. (b) Hill, R. J.; Long, D.-L.; Champness, N. R.; Hubberstey, P.; Schröder, M. *Acc. Chem. Res.* **2005**, *38*, 337. (c) Zeng, M. H.; Wang, B.; Wang, X. Y.; Zhang, W. X.; Chen, X. M.; Gao, S. *Inorg. Chem.* **2006**, *45*, 7069.

(8) Batten, S. R.; Robson, R. *Angew. Chem., Int. Ed.* **1998**, *37*, 1460.

(9) (a) Abrahams, B. F.; Hardie, M. J.; Hoskins, B. F.; Robson, R.; Sutherland, E. E. *J. Chem. Soc., Chem. Commun.* **1994**, 1049. (b) Carlucci, L.; Ciani, G.; Proserpio, D. M. *Coord. Chem. Rev.* **2003**, *246*, 247.

(10) Tong, M. L.; Chen, X. M.; Batten, S. R. *J. Am. Chem. Soc.* **2003**, *125*, 16170.

(11) (a) Wang, X.-L.; Qin, C.; Wang, E.-B.; Su, Z.-M.; Xu, L.; Batten, S. R. *Chem. Commun.*, **2005**, 4789. (b) Wang, X.-L.; Qin, C.; Wang, E.-B.; Su, Z.-M. *Chem. Eur. J.* **2006**, *12*, 2680.

Table 1. Summary of Crystal Data and Refinement Results

compounds	**1**^{c}	**2**^{c}	**3**^{c}	**1**^{a}	**2**^{a}	**3**^{a}
chemical formula	$C_{30}H_{36}Cu_2N_2O_8$	$C_{30}H_{36}Zn_2N_2O_8$	$C_{76}H_{86}Cd_4N_6O_{16}$	$C_{30}H_{36}Cu_2N_2O_8$	$C_{30}H_{36}Zn_2N_2O_8$	$C_{38}H_{43}Cd_2N_3O_8$
structural formula	Cu_2(D-Cam)$_2$ (4,4-bpy)	Zn_2(D-CAA)$_2$ (4,4-bpy)	Cd_4(D-CAA)$_4$ (bpe)$_3$	Cu_2(DL-Cam)$_2$ (4,4-bpy)	Zn_2(DL-Cam)$_2$ (4,4-bpy)	Cd_2(DL-CAA)$_2$ (bpe)$_{3/2}$
fw	679.69	683.35	1789.12	679.69	683.35	894.5
temp (K)	293	293	293	293	293	293
a (Å)	21.2692(16)	7.7559(19)	18.8494(7)	21.3215(6)	7.7316(9)	9.5125(3)
b (Å)	12.5647(6)	11.598(3)	10.8373(4)	12.6721(4)	11.688(1)	11.3212(3)
c (Å)	13.4995(10)	17.588(5)	19.0705(7)	13.4677(4)	17.204(2)	18.4446(4)
α (deg)	90	90	90	90	90	104.879(2)
β (deg)	121.843(2)	102.640(2)	102.786(2)	121.974(2)	101.228(4)	92.208(2)
γ (deg)	90	90	90	90	90	95.825(2)
V (Å^3)	3064.7(4)	1543.8(7)	3799.1(2)	3086.76(16)	1524.9(3)	1905.52(9)
Z	4	2	2	4	2	2
space group	$C2$	$P2_1$	$P2_1$	$C2/c$	$P2_1/n$	$P\bar{1}$
$2\theta_{max}$ (deg)	55	55	45	50	47	51
total data	11559	12165	21175	11913	8212	18957
unique data	6685 [R(int) = 0.0165]	5494 [R(int) = 0.0206]	8415 [R(int) = 0.0624]	2683 [R(int) = 0.0900]	2265 [R(int) = 0.0543	7066 [R(int) = 0.0696]
data, $I > 2\sigma(I)$	6211	4630	6693	1534	1591	4492
Flack parameter	0.013(13)	−0.019(16)	0.01(3)	N/A	N/A	N/A
$R(F)$ ($I > 2\sigma(I)$)	0.0402	0.0328	0.0352	0.0658	0.0521	0.0444
$R_w(F^2)$($I > 2\sigma(I)$)	0.1085	0.0865	0.0655	0.1505	0.1487	0.1004
GOF	1.030	1.086	0.904	1.037	1.053	0.937

Scheme 1. Six Coordination Modes of the D-Cam Ligands Observed in 1^{c} (a), 1^{a} (a), 2^{c} (b), 2^{a} (b), 3^{c} (c, d), and 3^{a} (e, f)

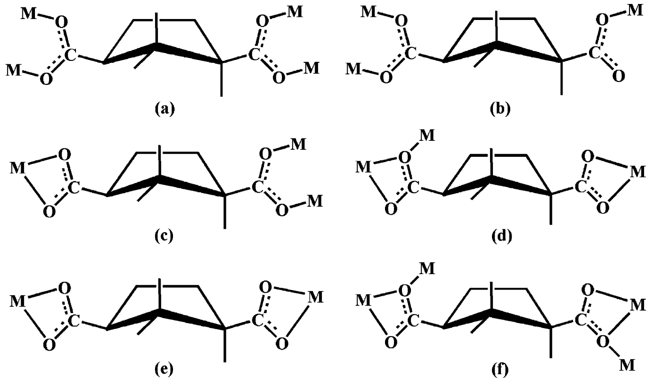

Fourier methods. All non-hydrogen atoms were refined anisotropically. Computations were performed using SHELXTL and final full-matrix refinements were against F^2. The crystallographic results are summarized in Table 1.

Results and Discussion

Homochiral **1**^{c}−**3**^{c} and racemic chiral **1**^{a}−**3**^{a} were obtained by hydrothermal synthesis. Single-crystal X-ray structure analysis shows that they all have polymeric structures based on networks of six-connected dinuclear metal clusters cross-linked by bridging enantiopure or racemic camphoric acid and bipyridine. They all contain metal carboxylate gridlike (4,4) layers and the replacement of racemic DL-Cam ligand by the enantiopure D-Cam ligand causes a conversion from racemic chiral structure to homochiral structure. The auxiliary bipyridine ligands act as pillars to cross-link the homchiral or racemic chiral metal-carboxylate sheets into non-interpenetrating 3-D architectures. However, depending on chemical compositions, the effect of ligand chirality can be quite different as described below. In addition, these materials exhibit unusual self-penetrating topology reminiscent of knot-type structures in molecular systems. Compounds **1**^{c} and **1**^{a} have the same topological type Figure 1 and nearly identical crystal structures, even though the chirality of ligands at 50% ligand sites is opposite. Compounds **2**^{c} and **2**^{a} exhibit an unprecedented topological type Figure 2 and also have nearly identical crystal structures. Compounds **3**^{c} and **3**^{a} have the same topology as **2**^{c} Figure 3. However, homochiral **3**^{c} has a 2-fold supercell compared with racemic chiral **3**^{a}. Homochiral layers in **3**^{c} and racemic chiral layers in **3**^{a} are pillared differently as described below.

Zero-Handedness Effect on Crystallization: Isostructural Racemic Chiral to Homochiral Conversion in Six-Connected Framework Materials. Despite the fundamental difference in chirality, compounds **1**^{c} and **1**^{a} have nearly identical unit cells and crystal structures. Because crystals structures prepared from enantiopure and racemic molecules are usually quite different, the isostructure observed for **1**^{c} and **1**^{a} is an interesting example that illustrates the minimal effect of the ligand handedness on the crystallization of chiral and racemic chiral frameworks from enantiopure or racemic ligand.

Compound **1**^{c} was prepared from enantiopure D-Cam and crystallized in the chiral space group $C2$ whereas **1**^{a} was prepared from racemic DL-Cam and crystallized in achiral space group $C2/c$. In **1**^{c}, the asymmetric unit contains two Cu atoms, two D-Cam ligands, and one 4,4′-bipy ligand. Each copper site has square pyramidal geometry (not considering the Cu...Cu linkage within the dimer) and the copper dimers are bridged by four bidentate carboxylate groups from four D-Cam ligands into a paddle-wheel unit with a metal−metal separation of 2.650(1) Å (Figure 1a, Scheme 1a). The D-Cam ligands join the dinuclear copper clusters into a homochiral gridlike (4,4) layered structure (Figure 1c).

In comparison, the asymmetric unit of **1**^{a} contains only one Cu atom, one Cam molecule, and half of a 4,4′-bipy ligand because of the presence of an additional symmetry element. The paddle-wheel-like dinuclear Cu unit is surrounded by two D-Cam ligands, two L-Cam ligands, and two 4,4′-bipy ligands (Figure 1b). The equal ratio between D- and L-Cam ligands in **1**^{a} creates a racemic chiral metal carboxylate gridlike (4,4) layer (Figure 1d).

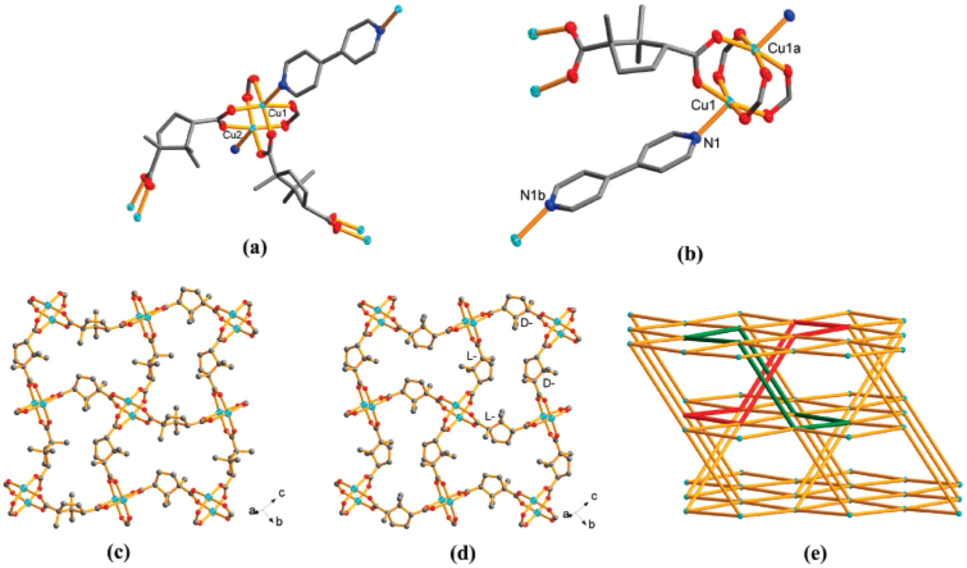

Figure 1. (a) Asymmetric unit in $\mathbf{1^c}$; (b) asymmetric unit in $\mathbf{1^a}$; (c) 2-D homochiral layer in $\mathbf{1^c}$; (d) 2-D achiral layer in $\mathbf{1^a}$; (e) view of the 4^86^68 topology (rob) of $\mathbf{1^c}$ and the self-catenated shortest circuits (green and red).

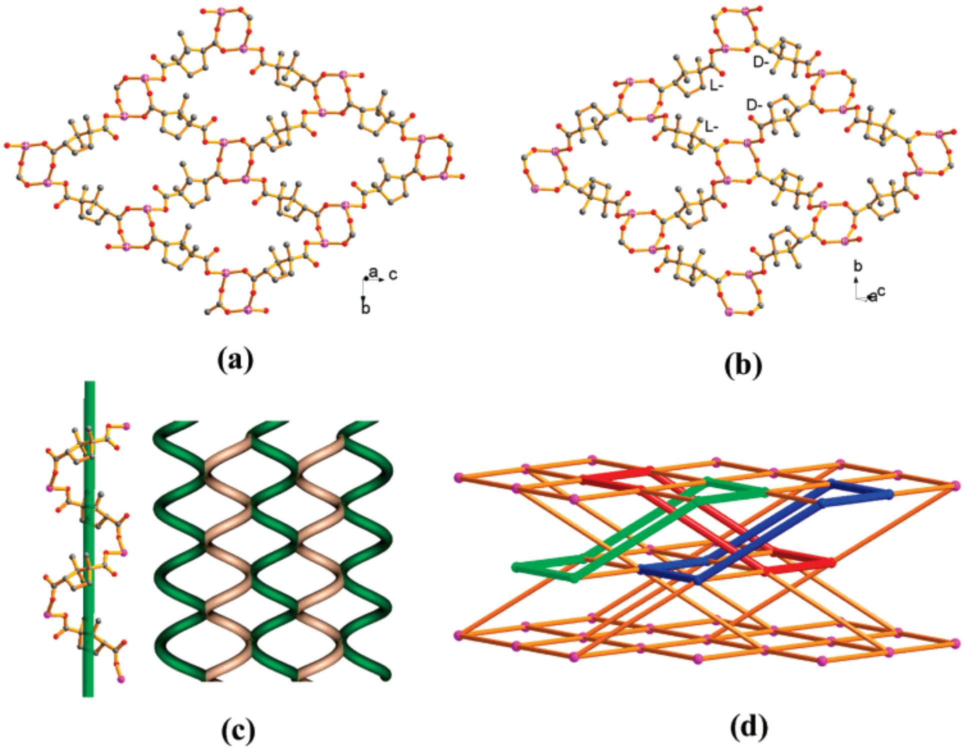

Figure 2. (a) Homochiral 2-D layer in $\mathbf{2^c}$; (b) achiral 2-D layer in $\mathbf{2^a}$; (c) 2_1 helix in $\mathbf{2^c}$ and the orderly arrangement of left- and right-handed helices; (d) view of the $4^46^{10}8$ topology (LB-1) of $\mathbf{2^c}$ and the self-catenated shortest circuits (green, blue, and red).

Each dinuclear copper cluster in $\mathbf{1^c}$ or $\mathbf{1^a}$ is connected to six other clusters through four Cam ligands and two 4,4′-bpy ligands to generate a neutral six-connected 3-D network with 4^86^68 topology (known as the rob type, Figure 1e).[7] One key feature of this topology is the cross-linking of 2-D (4,4) nets by parallel rods. Another interesting feature of this topology is the presence of self-catenation. In other words, its shortest circuits are penetrated by rods of the same network like in molecular knots. As highlighted in Figure 1e, two shortest six-membered circuits that serve to join together (4,4) nets form the catenane-like interlocking structure. To express such self-catenation in chemical terms, four D-Cam ligands and two 4,4′-bpy ligands connect six dinuclear copper clusters to form a large super-ring that are penetrated by another 4,4′-bpy ligand at its center (Figure 4a). There were two previous reports of a related topology.[7a,c] However, in both cases, octahedral transition metals (instead of clusters reported here) serve as six-connected nodes and there are no homochiral building blocks.

An interesting observation about $\mathbf{1^c}$ and $\mathbf{1^a}$ is the nearly identical unit cell parameters between the chiral $\mathbf{1^c}$ and racemic chiral $\mathbf{1^a}$ forms. In other words, we have demonstrated that it is possible to replace every other enantiopure D-Cam ligands with the opposite L-Cam ligands and yet still

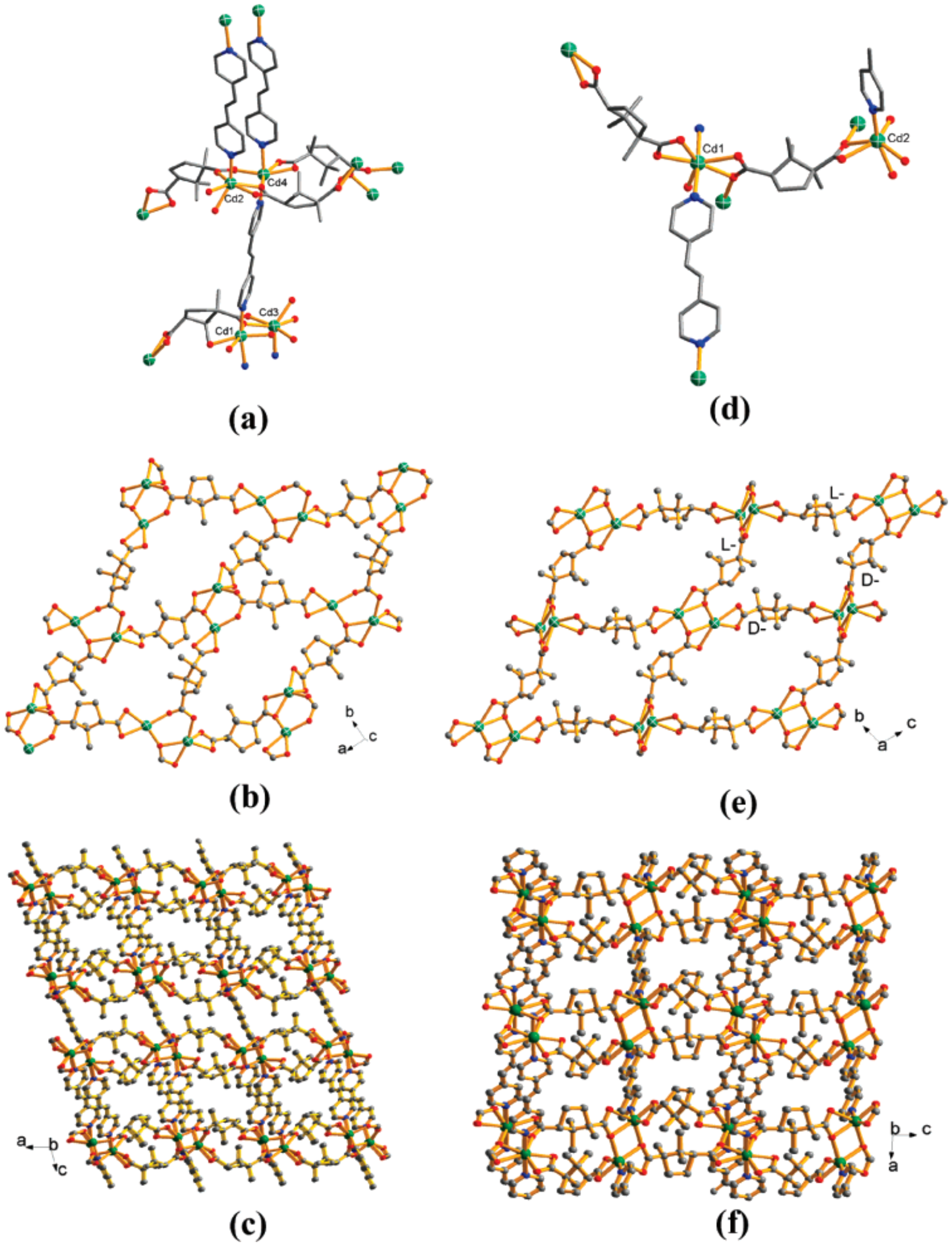

Figure 3. (a) Asymmetric unit in **3**$^{\mathbf{c}}$; (b) homochiral 2-D layer in **3**$^{\mathbf{c}}$; (c) homochiral 3-D framework of **3**$^{\mathbf{c}}$, showing single pillars and double pillars in the laternating fashion; (d) asymmetric unit in **3**$^{\mathbf{a}}$; (e) achiral 2-D layer in **3**$^{\mathbf{a}}$; (f) achiral 3-D framework of **3**$^{\mathbf{a}}$, showing mixed single and dual pillars in the same interlayer regions.

maintain the same crystal structure. There is little change in six dimensions of unit cell parameters. It is worth noting that crystals obtained from enantiopure ligands and racemates generally have different crystal structures because of the differing symmetry requirements.

Isostructural Homochiral and Racemic Chiral Frameworks with Previously Unknown Topology. When Zn(NO$_3$)$_2$·6H$_2$O was used instead of Cu(NO$_3$)$_2$·3H$_2$O, the isostructural compounds **2**$^{\mathbf{c}}$ and **2**$^{\mathbf{a}}$ with a previously unknown topology were obtained. Such a topological change is primarily due to the different coordination chemistry between Cu^{2+} (square-pyramidal in **1**$^{\mathbf{c}}$ and **1**$^{\mathbf{a}}$) and Zn^{2+} (tetrahedral in **2**$^{\mathbf{c}}$ and **2**$^{\mathbf{a}}$). **2**$^{\mathbf{c}}$ and **2**$^{\mathbf{a}}$ also have the nearly identical unit cell parameters between the chiral **2**$^{\mathbf{c}}$ and racemic chiral **2**$^{\mathbf{a}}$ forms. The asymmetric unit in **2**$^{\mathbf{c}}$ contains two Zn atoms, two D-Cam ligands, and one 4,4′-bipy ligand, while the asymmetric unit in **2**$^{\mathbf{a}}$ contains only half of them. Each tetrahedral Zn site is coordinated by three carboxylate oxygen atoms from three Cam ligands and one nitrogen atom of a 4,4′-bpy ligand. Each Cam ligand uses one bidentate carboxylate group to bridge two metal sites and the other monodenate carboxylate group to bond to a single metal site (Figures 2a and 2b and Scheme 1b). The nonbonding metal−metal distances within the dinuclear cluster are 3.823 Å in **2**$^{\mathbf{c}}$ and 3.750 Å in **2**$^{\mathbf{a}}$.

The homochiral layer in **2**$^{\mathbf{c}}$ consists of 2_1 helical chains along the *b*-axis (Figure 2c). The helical chain is formed by alternating D-Cam ligands and metal sites. The left- and right-handed helices are joined together through the common dinuclear metal clusters. Although the ratio between the left-

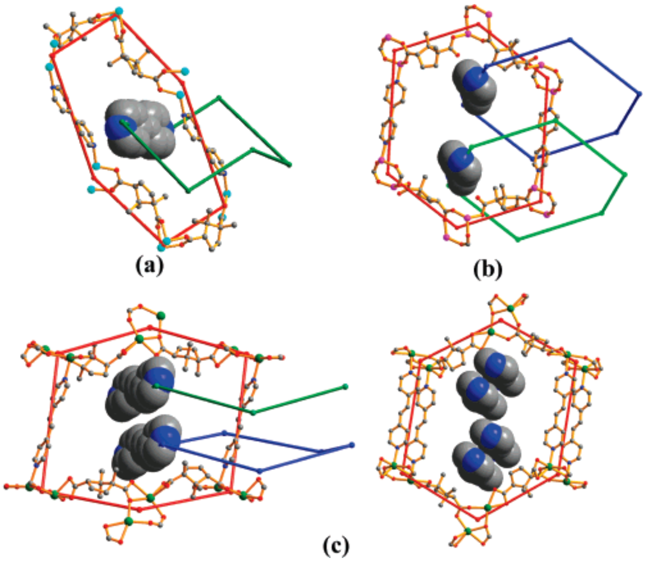

Figure 4. Illustration of self-penetration in **1**^{c}, **2**^{c}, and **3**^{c}. (a) In **1**^{c}, one 4,4′-bpy ligand is located in the ring; (b) in **2**^{c}, two 4,4′-bpy ligands are located in the ring; (c) in **3**^{c}, two bpe ligands are located in a ring and four bpe ligands are located in another ring.

and right-handed helices is 1:1, the resulting 3-D framework is homochiral because of the presence of the enantiopure building block.

To our knowledge, the network topology exhibited by **2**^{c} (denoted the LB-1 net here) has not been seen in other compounds. In **2**^{c}, the 4,4′-bpy ligands link dinuclear clusters to form chains that are tilted with respect to the homochiral metal-carboxylate layer. However, the interlayer distance is 7.756 Å, significantly shorter than the corresponding distance of 8.894 Å in **1**^{c}, indicating a higher degree of tilting of 4,4′-bpy in **2**^{c}. The Schläfli symbol for the net in **2**^{c} is $4^46^{10}8$. Within this net, each shortest six-membered ring is catenated by two rods of the same network (Figure 2d), which indicates that it is a self-penetrating net. A structural illustration of the catenane-like configuration is given in Figure 4b, and two 4,4′-bpy ligands are shown to occupy the large space around the center of the large super-ring.

Racemic Chiral to Homochiral Conversion Accompanied by Supercell Formation and a Change in the Pillaring Pattern. Unlike the isostructural racemic chiral to homochiral conversion between **1**^{c} and **1**^{a}, **2**^{c} and **2**^{a}, the use of the enantipure and racemic camphoric acid together with Cd^{2+} and *trans*-1,2-bis(4-pyridyl)-ethylene gives homochiral **3**^{c} and racemic chiral **3**^{a} with distinct unit cells and crystal structures.

In **3**^{c}, the asymmetric unit contains four independent Cd atoms, four D-Cam ligands, and three bpe ligands (Figure 3a). Six-coordinate Cd sites exhibit two types of connectivity to ligands: $[CdO_5N]$ and $[CdO_4N_2]$. In addition, there are two types of bonding modes between Cd sites and D-Cam as shown in Schemes 1c and 1d. A dinuclear Cd cluster is formed with two oxygen sites of a bidentate carboxylate group and one oxygen site from another D-Cam ligand. Similar to **2**^{c}, the D-Cam ligands bridge the dinuclear Cd cluster to generate a gridlike (4,4) layer with 2_1 helices (Figure 3b). The resulting layers are further pillared by bpe ligands, giving rise to a 3-D framework (Figure 3c).

Scheme 2. Schematic Representation of the Pillared Layered Structures in 3^{c} and 3^{a}, Respectively

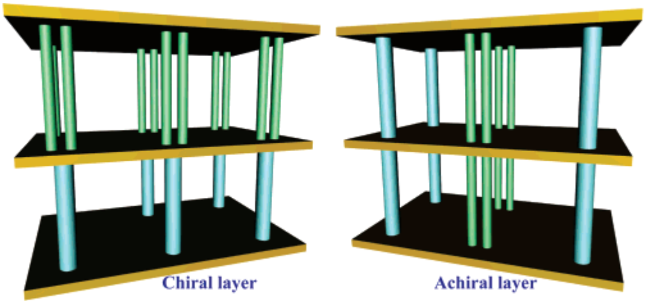

In **3**^{a}, the asymmetric unit contains two Cd atoms, two Cam ligands, and one and half bpe ligands (Figure 3d). The Cd1 atom is seven-coordinate to five O atoms from three different Cam ligands and two N atoms from two bpe ligands. The Cd2 atom is six-coordinate to five O atoms from three different Cam ligands and one N atom from one bpe ligands. Two symmetry-related Cd atoms are bridged by two carboxylate groups to form a dinuclear Cd cluster.

An interesting difference between **3**^{c} and **3**^{a} is the different way in which chiral layers in **3**^{c} and racemic chiral layers in **3**^{a} are pillared by bipyridine ligands (Scheme 2). In both **3**^{c} and **3**^{a}, there are two types of pillars: single pillar (one bpe ligand between two dinuclear Cd clusters) and double-pillar (two bpe ligands between two dinuclear Cd clusters). In **3**^{a}, both single and dual pillars exist within the same interlayer region (Figure 3f). In other words, any two adjacent achiral layers in **3**^{a} are pillared by a 50:50 mixture of single and dual pillars and the periodicity along the layer stacking direction corresponds to just one interlayer distance. In contrast, compound **3**^{c} has a 2-fold supercell compared to **3**^{a}. In **3**^{c}, only one type of pillars (either single or dual) is observed in the same interlayer region (Figure 3c). Two adjacent chiral layers are joined together by single pillars in one interlayer region and by dual pillars in the next interlayer region along the layer stacking direction. Therefore, the periodicity along the layer stacking direction in **3**^{a} corresponds to two interlayer distances.

Topological Relationship among Six-Connected 3-D Frameworks. All five compounds reported have unusual six-connected self-penetrating networks. Compounds **1**^{c} and **1**^{a} exhibit the *rob* type topology that is already known in the literature while compounds **2**^{c}, **2**^{a}, **3**^{c}, and **3**^{a} exhibit LB-1 type topology. There is an interesting relationship between LB-1 ($4^46^{10}8$) net and other six-connected nets: pcu ($4^{12}6^3$), roa ($4^46^{10}8$), and rob (4^86^68): they are all six-connected nets based on (4,4) 2-D sheets.

In an ideal pcu net, the pillars are perpendicular to the (4,4) 2-D sheet, while in roa, rob, and LB-1 nets, the pillars are titled with respect to the (4,4) sheet. The roa, rob, and LB-1 nets are all self-penetrating nets, but have different degrees of catenation. As shown in Scheme 3, the catenation in the rob net involves two six-membered rings (1 + 1), and the catenation in LB-1 net involves three six-membered rings (1 + 2). The catenation in roa net involves four six-membered rings (1 + 3). The LB-1 net and the roa net have the same schläfli symbol ($4^46^{10}8$), but their coordination

Scheme 3. View of Three Types of Catenations in the rob, LB-1, and roa Nets, Respectively

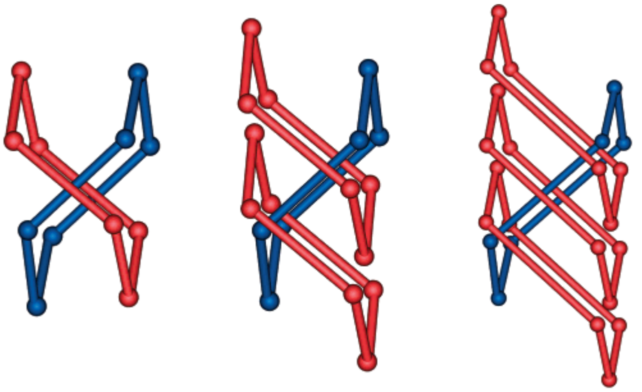

Catenation in rob net Catenation in LB-1 net Catenation in roa net

sequence (cs) and vertex symbol (vs) are different. For the roa net,[5d] the vertex symbol is $4.4.4.4.6_2.6_2.6_5.6_5.6_5.6_5.6_5.6_5.6_5.6_5.*$. The topological analysis of the LB-1 has been performed using the Systre[12] and OLEX[13] programs. The maximum symmetry of the LB-1 net is orthorhombic *Pmna* and its vertex symbol is $4.4.4.4.6_4.6_4.6_5.6_5.6_5.6_5.6_{11}.6_{11}.6_{11}.6_{11}.*$.

Conclusion

Hydrothermal synthesis, crystal structure, and topological properties of three homochiral and three racemic chiral framework materials are reported here. These materials have rather rare homochiral six-connected self-penetrating topology. The framework topology is based on the pillaring of gridlike homochiral or racemic chiral layers pillared by bipyrdine ligands. An interesting isostructural transformation from a racemic chiral framework to a chiral framework has been achieved for the six-connected structure by employing enantiopure and racemic mixtures, further demonstrating the feasibility and general applicability of direct conversion from an achiral framework to a homochiral framework through ligand design. Furthermore, a different achiral−chiral conversion has also been observed in which homochiral layers are pillared by either all single pillars or all dual pillars within the same interlayer region whereas achiral layers are pillared by a mixture of single and dual pillars within the same interlayer region.

Acknowledgment. We are thankful for the support of this work by the National Institutes of Health (2 S06 GM063119-05).

Supporting Information Available: TGA results and crystallographic data including positional parameters, thermal parameters, and bond distances and angles (PDF); crystallographic information in CIF format. This material is available free of charge via the Internet at http://pubs.acs.org.

CM071689A

---

(12) (a) Delgado-Friedrichs, O.; O'Keeffe. M. *Acta Crystallogr.* **2003**, *A59*, 351. (b) Delgado-Friedrichs, O. *Discr. Comput. Geom.* **2005**, *33*, 67.

(13) Dolomanov, O. V.; Blake, A. J.; Champness, N. R.; Schröder, M. *J. Appl. Crystallogr.* **2003**, *36*, 1283.